Operator Spectrum and Exact Exponents of the Fully Packed Loop Model

Kondev, J.; de Gier, J.C.; Nienhuis, B.

DOI
10.1088/0305-4470/29/20/007
Publication date
1996

Published in
Journal of Physics. A, Mathematical and General

J. Phys. A: Math. Gen. **29** (1996) 6489–6504. Printed in the UK

Operator spectrum and exact exponents of the fully packed loop model

Jané Kondev†, Jan de Gier‡ and Bernard Nienhuis‡

† Department of Physics, Brown University, Providence, Rhode Island 02912-1843, USA
‡ Instituut voor Theoretische Fysica, Universiteit van Amsterdam, Valckenierstraat 65, 1018 XE Amsterdam, The Netherlands

Received 25 March 1996, in final form 17 June 1996

Abstract. We develop a Coulomb-gas description of the critical fluctuations in the fully packed loop model on the honeycomb lattice. We identify the complete operator spectrum of this model in terms of electric and magnetic *vector* charges, and we calculate the scaling dimensions of these operators exactly. We also study the geometrical properties of loops in this model, and we derive exact results for the fractal dimension and the loop-size distribution function. A review of the many different representations of this model that have recently appeared in the literature, is given.

1. Introduction

Loop models, loosely speaking, are statistical models which have as basic building blocks loops that run along the bonds of a two-dimensional lattice. In order to define a loop model one assigns Boltzmann weights to the different loop configurations. This is usually implemented by assigning weights to the different vertex configurations allowed by the loop model, and a weight to the loop as a whole; this loop weight is usually referred to as the fugacity.

Loop models have attracted attention recently as representations of certain exactly solvable vertex models which can be used to construct restricted solid-on-solid models [1], some of which admit an off-critical extension [2]. They are also particularly simple examples of models that allow for Monte Carlo simulations with non-local loop updates, which have been recently studied as algorithms that reduce critical slowing down [3]. In a completely different setting, loop models appear as spacetime diagrams in the path integral representation of one-dimensional quantum spin chains, and many quantities defined in terms of the spins can be re-expressed in the language of loops [4]. For instance, it can be shown that the spin–spin correlation function in the antiferromagnetic Heisenberg spin chain, is given by the loop correlation function in the appropriate loop model [4]. The loop correlation function measures the probability that two points on the lattice belong to the same loop.

In two-dimensional classical spin models loops are typically encountered as domain boundaries, e.g. Bloch walls in the Ising model, or as graphical representations of high-temperature expansions. Recently, Cardy [5] has calculated different geometrical properties of cluster boundaries in the O(n) model on the honeycomb lattice, using the loop representation of this model.

0305-4470/96/206489+16$19.50

In this paper we study the fully packed loop (FPL) model on the honeycomb lattice. The FPL model was introduced by Reshetikhin [6], and independently by Blöte and Nienhuis [7], as the zero-temperature limit of the O(n) model. Using numerical transfer-matrix methods, Blöte and Nienhuis were able to to show that this loop model defines a universality class distinct from the previously studied low-temperature phase of the O(n) model. Exact values of the critical exponents and the conformal charge of the FPL model were subsequently determined by Batchelor *et al* [8], who found a Bethe ansatz solution of the model.

In the FPL model non-intersecting loops are placed along the bonds of a honeycomb lattice so that *every* vertex of the lattice is covered by a loop. The partition function is given by

$$Z_{FPL} = \sum_{\mathcal{G}} n^{N(\mathcal{G})} \tag{1}$$

where N is the number of loops in the fully packed configuration $\mathcal{G}$, and n is the loop fugacity.

This model undergoes a phase transition as a function of the loop fugacity n. For values of n approaching zero, configurations with a small number of big loops are favoured; in the limit $n \to 0$ a single loop covers the whole lattice†. Loops of all sizes will be present on the lattice as we increase n. This is equivalent to having a diverging correlation length in the system [9], and the model is critical with power law correlations. At $n = 2$ the FPL model undergoes a Kosterlitz–Thouless type of transition [6, 10] into a long-range ordered state, in which there exists a largest loop on the lattice which is roughly the size of the correlation length. In the $n \to \infty$ limit the fully packed loop model is perfectly ordered, with all the loops having the minimal length of six, and occupying one of the three sublattices of hexagonal plaquettes.

Here we turn our attention to the FPL model along the critical line ($0 \leqslant n \leqslant 2$), which was also the focus of the above-mentioned numerical transfer-matrix study, and of the Bethe ansatz solution. Using a nested Bethe ansatz Batchelor *et al* [8] calculated the scaling dimensions of the 'watermelon' operators along the critical line. The watermelon correlation function is defined as the probability that m loop segments meet in the neighbourhood of two points separated by $\boldsymbol{r}$ [11]. Here we rederive the same results from a Coulomb gas approach in which the loop model is mapped to an interface model. In the interface representation 'watermelon' scaling dimensions become associated with vortices whose topological charges are vectors in the triangular lattice. Furthermore, this approach allows us to identify the *complete* operator spectrum of the FPL model and make contact with known results from conformal field theory. In particular, we calculate exactly the temperature dimension found numerically by Blöte and Nienhuis [7], that does not appear in the Bethe ansatz solution of Batchelor *et al* [8]. We also identify defect configurations in the loop model that generalize the 'watermelon' configurations, and we calculate the critical exponents associated with them.

The main shortcoming of the Coulomb-gas approach, in general, is that it usually relies on some exact information about the model which is used to calculate the value of the renormalized coupling [12]. Once the coupling is known all the exponents can be calculated exactly. We will show that in the FPL model the coupling can be determined exactly by identifying the marginal operators in this model. The existence of these operators is required by certain consistency conditions placed on conformal field theories which describe the scaling limits of lattice models; this was discussed at length by Dotsenko and Fateev [13].

† This limit was studied by Batchelor *et al* [8] who obtained exact results for Hamiltonian walks on the honeycomb lattice.

Many of our results for the critical exponents of the FPL model have been found previously from a Bethe ansatz solution [8]. Our main motivation for pursuing the Coulomb-gas approach is its relative simplicity, and the geometrical interpretation of the operator spectrum of the FPL model, which it offers. Furthermore, this approach allows us to identify the conformal field theory that describes the scaling limit of the FPL model, which can then be used to study the critical properties of this model in detail, using the many conformal techniques at our disposal.

This paper is organized as follows. In section 2 we have collected the different known representations of the FPL model, and mappings from one to the other are made explicit. In section 3 we introduce an effective-field theory of the FPL model, and section 4 is devoted to the construction of the associated Coulomb gas and the calculation of the scaling dimensions of different operators. These results are used in section 5 to calculate the geometrical exponents for loops in the FPL model.

2. Representations of the FPL model

The FPL model has many different representations, some of which have been independently studied. Here we review the mappings between the different representations.

The FPL model is equivalent to the three-colouring model on the honeycomb lattice introduced by Baxter [14]. The three-colouring model is defined by colouring the bonds of the honeycomb lattice with three different colours, say A, B, and C, in such a way that no two bonds of equal colour meet at a vertex†. For $n = 2$ each colouring is given equal statistical weight. If we choose any two colours, say B and C, then the bonds coloured with these two colours form a fully packed loop configuration on the honeycomb lattice. Each loop can be coloured with alternating colours B and C in two ways (B-C-B ... or C-B-C ...), and is therefore assigned a fugacity $n = 2$. The FPL model away from the $n = 2$ point can also be mapped to a colouring model, but now the weights of the different colourings will have to be modified; see section 4.2.

If we consider the three colours as Potts spins placed at the centres of the bonds of the honeycomb lattice, then the three-colouring model describes the ground state of the three-state antiferromagnetic Potts model on the Kagomé lattice studied by Huse and Rutenberg [15]. The Potts model is defined by the Hamiltonian (energy functional)

$$H = |J| \sum_{\langle ij \rangle} \delta_{\sigma_i, \sigma_j} \tag{2}$$

where the sum goes over nearest neighbours, and the spins σ_i live on the vertices of the Kagomé lattice. At zero temperature the only allowed states are ones where on every triangular plaquette all three spins are unequal. This ground state manifold is critical in the sense that correlation functions of the spins decay with distance as power laws [15].

The three-colouring model can be mapped to a solid-on-solid model that describes a two-dimensional interface in *four* spatial dimensions [15, 10]. This is accomplished by placing a two-component microscopic height $\boldsymbol{z}$ at the centre of each plaquette of the honeycomb lattice; see figure 1. The change in $\boldsymbol{z}$ when going from one plaquette to the neighbouring one is given by $\boldsymbol{A}$, $\boldsymbol{B}$, or $\boldsymbol{C}$, depending on the colour of the bond that is crossed; the vectors $\boldsymbol{A}$, $\boldsymbol{B}$, and $\boldsymbol{C}$ point to the vertices of an equilateral triangle,

$$\boldsymbol{A} = \left(\frac{1}{\sqrt{3}}, 0\right) \qquad \boldsymbol{B} = \left(-\frac{1}{2\sqrt{3}}, \frac{1}{2}\right) \qquad \boldsymbol{C} = \left(-\frac{1}{2\sqrt{3}}, -\frac{1}{2}\right) \tag{3}$$

† These type of graph colourings are known in the mathematics literature as *edge colourings*.

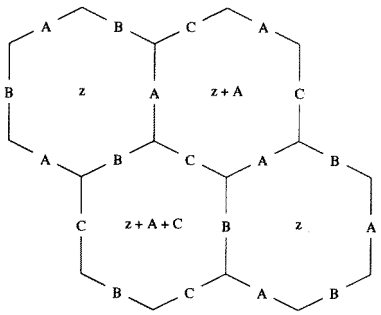

Figure 1. One of six symmetry-related ideal states of the three-colouring model. In an ideal state all the plaquettes are coloured with two colours only. The microscopic heights z are defined at the centres of the plaquettes, and the change in z, when going from one plaquette to the neighbouring one, is determined by the colour of the crossed bond. The ideal state is macroscopically flat, in the sense that the variance of the microscopic height is minimal.

where we have chosen the normalization for later convenience. We also adopt the convention that one of the vectors $\boldsymbol{A}$, $\boldsymbol{B}$, or $\boldsymbol{C}$ is *added* to the microscopic height when going clockwise around an up-pointing triangle of the dual lattice (i.e. around a vertex of the honeycomb lattice in the shape of the letter Y); see figure 1. Up to an arbitrary choice of a single height, say at the origin, the mapping of the colouring to the heights is one to one. Each allowed height configuration is given equal statistical weight.

It has been recently shown by Di Francesco and Guitter [16] that the three-colouring model can be mapped to a folding model of the triangular lattice, introduced by Kantor and Jarić [17]. The allowed configurations in the folding model are given by all the possible *complete* foldings of the triangular lattice†. A folding configuration can be specified by giving the direction (+ or − in the third dimension) of the normal to each elementary triangle in the folded state. Now if we place the three colours, A, B, and C, on the bonds of every elementary triangle in a clockwise (+) or anticlockwise (−) fashion we obtain a three-colouring configuration of the dual honeycomb lattice. This is a six-to-one mapping, since for a given folded configuration one is free to choose one of six colour configurations around a single triangle, which then fixes all the rest.

3. Effective-field theory

In this section we propose an effective-field theory for the long wavelength fluctuations of the interface model, which is one of the representations of the FPL model discussed in the previous section. Here we focus on the $n = 2$ case which is equivalent to the three-colouring model with equal statistical weight for all the colourings, and extend to $n < 2$ in the following section.

We motivate the long-wavelength theory of the interface model by a coarse-graining procedure of the microscopic heights $\boldsymbol{z}$, which is implemented as follows‡. First, we define the *ideal states* which we use to coarse-grain the three-colouring model. Ideal states are edge-colouring states in which every elementary plaquette of the honeycomb lattice

† This model is a special case of a more general folding model due to Shender *et al* [18], which is equivalent to the ground states of the antiferromagnetic *Heisenberg* model on the Kagomé lattice.

‡ More details of the height construction for the $n = 2$ FPL model, as well as for other critical ground states, can be found in [19].

is coloured with two colours only; figure 1. These states are flat, in the sense that they minimize the variance of the microscopic height, and we argue that the free energy of the colouring model† is dominated by fluctuations around the ideal states. Namely, the smallest change on the lattice, that is allowed by the constraints of the three-colouring model, is an exchange of colours along a *loop* of alternating colour (e.g. C-B-$C\ldots$ to B-C-$B\ldots$). The ideal states *maximize* the number of loops that allow for these loop exchanges, and it is this property that selects them out. This entropic selection effect is close in spirit to the 'order by disorder' effect introduced by Villain [20]. In the FPL model ideal states are the ones selected in the $n \to \infty$ limit, while in the folding model these are states where the triangular lattice has been folded to a single triangle.

Second, we divide the honeycomb lattice into domains so that each domain represents a different ideal (flat) state. To each domain we assign a *coarse-grained height* $\boldsymbol{h}$, which is equal to the microscopic height averaged over the domain: $\boldsymbol{h} = \langle \boldsymbol{z} \rangle$.

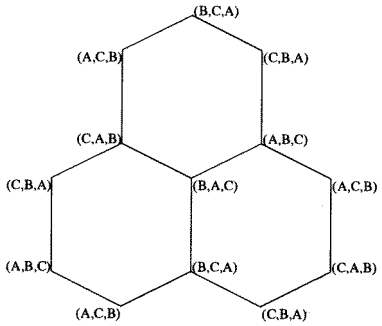

Figure 2. The ideal state graph of the three colouring model is a honeycomb lattice in height space: each vertex is associated with a particular ideal state, and the six different ideal states form a hexagonal plaquette. The ideal states are labelled by the colour configuration $(\sigma_1, \sigma_2, \sigma_3)$ of the bonds around a common vertex of the coloured lattice. The vertices in the ideal state graph that correspond to the *same* ideal state (say (C, B, A)) form a triangular lattice which is the *repeat* lattice of the three-colouring model.

The coarse-grained heights associated with the six different ideal states (one for every permutation of the three colours) form a honeycomb lattice which we call the *ideal state graph* $\mathcal{I}$; see figure 2. The side of the elementary hexagon of $\mathcal{I}$ is $\frac{1}{3}$, in the units chosen for the vectors representing the colours in equation (3). Nodes of $\mathcal{I}$ that correspond to the *same* ideal state form a triangular lattice with an elementary triangle of side 1. This lattice we call the *repeat* lattice $\mathcal{R}$; in the following section we will show that vectors $\boldsymbol{b} \in \mathcal{R}$ are the magnetic vector charges of the Coulomb gas associated with the FPL model.

Finally, we consider the continuum limit of the interface model in which the discrete heights, defined over different ideal-state domains, are replaced with a continuously varying height field $\boldsymbol{h}(\boldsymbol{r}) \equiv (h_1(\boldsymbol{r}), h_2(\boldsymbol{r}))$. The dimensionless free energy f of the interface, which is entropic in origin, is assumed to be of the form

$$f = \int \mathrm{d}^2\boldsymbol{r}\,[\pi g(|\nabla h_1|^2 + |\nabla h_2|^2) + V(\boldsymbol{h})] \tag{4}$$

where $2\pi g$ is usually referred to as the *stiffness*. $V(h)$ is a periodic potential with the

† The free energy of the three-colouring model is purely entropic in origin, in the sense that the partition function is simply equal to the number of different edge colourings.

periodicity given by the ideal state graph, i.e.

$$V(\mathbf{h}+\mathcal{I}) = V(\mathbf{h}). \tag{5}$$

The free energy f defines the (Euclidean) action of effective field theory of the three-colouring model; the assumption being made is that it correctly describes the long-wavelength fluctuations of the microscopic height $\boldsymbol{z}$. The periodic potential $V(\boldsymbol{h})$, which is usually referred to as the *locking potential*, favours the heights to take their values on $\mathcal{I}$, while the first term is the contribution to the free energy due to fluctuations around the flat ideal states. Therefore, the assumption that the effective-field theory of the three-colouring model is given by equation (4) is directly related to the intuitive idea put forward earlier, that the free energy of the three-colouring model is dominated by fluctuations around the ideal states.

The locking potential is periodic with the periodicity of $\mathcal{I}$. Thus, the three-colouring model, in its interface representation, undergoes a roughening transition for some value of the coupling $g = g_{\mathrm{r}}$ [21]. If the coupling g satisfies $g < g_{\mathrm{r}}$, then the locking potential in equation (4) becomes irrelevant, in the renormalization group sense, and the three-colouring model is described by a Gaussian model with an action

$$f = \pi g \int \mathrm{d}^2\boldsymbol{r}\,(|\nabla h_1|^2 + |\nabla h_2|^2). \tag{6}$$

In the case that the locking potential is relevant ($g > g_{\mathrm{r}}$), the three-colouring model will lock into long-range order in one of the ideal states. This would imply a finite correlation length in the FPL model, roughly the size of the largest loop in the system. We will see in the following section that for the three-colouring model which is equivalent to the $n = 2$ FPL model, g is *equal* to g_{r}, so the interface is *at* the roughening transition (i.e. the locking potential is *marginal*). For values of the fugacity $n < 2$ it will be shown that $g < g_{\mathrm{r}}$, but due to the presence of the background charge the chirality operator, which is related to the locking potential, remains marginal†.

4. Coulomb Gas

Here we develop the Coulomb-gas description of the FPL model based on its interface representation. We determine the spectrum of possible electric and magnetic charges and we calculate the scaling dimensions of operators associated with them. These are compared to recent numerical results [7], and to results from a Bethe ansatz solution of the FPL model [8]. We first consider the $n = 2$ FPL model which is described by a simple Gaussian-field theory, equation (6). The $n < 2$ case is treated by perturbing the $n = 2$ theory with an integrably marginal operator [23], and introducing a background charge in the Coulomb gas [13].

4.1. FPL model at $n = 2$

In constructing the effective-field theory of the three-colouring model, which maps to the $n = 2$ FPL model, we found that the height field $\boldsymbol{h}$ is compactified on the triangular lattice $\mathcal{R}$. Therefore, any local lattice operator $\Phi(\boldsymbol{r})$ which is uniform in the ideal states is periodic in height space, and it can be expanded into a Fourier series

$$\Phi(\boldsymbol{r}) = \sum_{\boldsymbol{G}\in\mathcal{R}^*} \Phi_{\boldsymbol{G}} \mathrm{e}^{\mathrm{i}2\pi \boldsymbol{G}\cdot\boldsymbol{h}(\boldsymbol{r})}. \tag{7}$$

† This seems to be a general property of critical loop models in two dimensions [22].

Here $\mathcal{R}^*$ is the lattice dual to $\mathcal{R}$, i.e. $\boldsymbol{G}\cdot\boldsymbol{b} \in \mathbb{Z}$ for any two vector charges $\boldsymbol{b} \in \mathcal{R}$ and $\boldsymbol{G} \in \mathcal{R}^*$. The Gaussian-field theory, equation (6), describes the vacuum phase of a two-dimensional Coulomb gas of electric ($\boldsymbol{G}$) and magnetic ($\boldsymbol{b}$) vector charges [12].

The scaling dimension of $\Phi(\boldsymbol{r})$ is equal to the scaling dimension of the most relevant *vertex* operator $\exp(\mathrm{i}2\pi\boldsymbol{G}\cdot\boldsymbol{h}(\boldsymbol{r}))$ appearing in its Fourier expansion. The scaling dimension $x(\boldsymbol{G})$, of a vertex operator, can be easily determined from its two-point correlation function,

$$\langle \mathrm{e}^{\mathrm{i}2\pi\boldsymbol{G}\cdot\boldsymbol{h}(\boldsymbol{r})}\mathrm{e}^{-\mathrm{i}2\pi\boldsymbol{G}\cdot\boldsymbol{h}(0)}\rangle \sim r^{-2x(\boldsymbol{G})}. \tag{8}$$

Namely, using a general property of a Gaussian distributed random field

$$\langle \mathrm{e}^{\mathrm{i}2\pi\boldsymbol{G}\cdot\boldsymbol{h}(\boldsymbol{r})}\mathrm{e}^{-\mathrm{i}2\pi\boldsymbol{G}\cdot\boldsymbol{h}(0)}\rangle = \mathrm{e}^{-\frac{1}{2}\langle[2\pi\boldsymbol{G}\cdot(\boldsymbol{h}(\boldsymbol{r})-\boldsymbol{h}(0))]^2\rangle} \tag{9}$$

and the height–height correlation function calculated in the Gaussian-field theory defined by equation (6) (for $r \gg a$; a is the lattice spacing)

$$\langle (h_i(\boldsymbol{r}) - h_j(0))^2\rangle = \text{constant} + \frac{\delta_{ij}}{2\pi^2 g}\ln|\boldsymbol{r}| \tag{10}$$

we find:

$$x(\boldsymbol{G}) = \frac{1}{2g}|\boldsymbol{G}|^2. \tag{11}$$

Operators with a non-zero magnetic charge $\boldsymbol{b} \in \mathcal{R}$ can be associated with a vortex configuration of the height field, or a violation of the edge-colouring constraint in the three-colouring model; see figure 3. The topological charge of the vortex is given by $\boldsymbol{b}$, i.e. the height mismatch around a vertex of the honeycomb lattice, and it can be calculated using the height rule introduced in section 3.

For a magnetic-type operator the scaling dimension $x(\boldsymbol{b})$ follows from the expression for the (dimensionless) interaction energy of a vortex–antivortex pair [12] (for $r \gg a$)

$$E_{\mathrm{int}} = g|\boldsymbol{b}|^2 \ln r + \text{constant}. \tag{12}$$

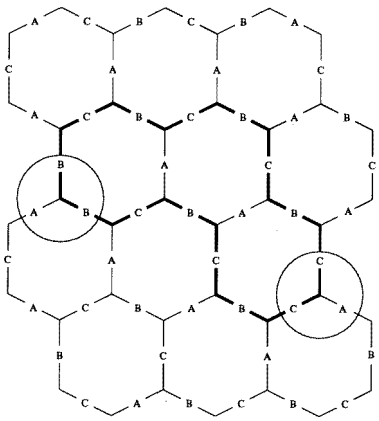

Figure 3. Elementary defects in the three-colouring model are associated with loops of alternating colour: exchanging the two colours (B and C) along one half of the loop (shown in bold) will generate defects (circled), that is violations of the edge colouring constraint, at the two ends. In the interface representation these defects become vortex–antivortex configurations of the height.

Here $\pm\boldsymbol{b}$ are the topological charges of the vortices and r is the distance between them; the above expression for $E_{\rm int}$ follows from the Gaussian form of the action, equation (6), and is simply the two-dimensional version of Coulomb's law. The vortex–antivortex correlation function is given by the Boltzmann factor

$$\mathrm{e}^{-E_{\rm int}} \sim r^{-2x(\boldsymbol{b})} \tag{13}$$

where $x(\boldsymbol{b})$ is fixed by the coupling g,

$$x(\boldsymbol{b}) = \frac{g}{2}|\boldsymbol{b}|^2. \tag{14}$$

Equations (11) and (14) specify the complete spectrum of scaling dimensions in the $n = 2$ FPL model. Next we turn to the problem of *identifying* specific correlation functions in this model associated with these exponents.

The dimension x_2, computed by Blöte and Nienhuis [7], governs the probability that two points on the honeycomb lattice lie on the same loop of the FPL model. The loops in the $n = 2$ FPL model are *contour* loops of a particular component of the height field. This is an important observation which will allow us to calculate the exact value of the coupling g, and we clarify it further.

Say we choose the BC loops in the three-colouring model to represent the loops in the FPL model. Now consider the points at the centres of the hexagonal plaquettes along one side of a BC loop. These points are separated by A coloured bonds, and consequently the component of the microscopic height $\boldsymbol{z}$ orthogonal to $\boldsymbol{A}$ is unchanged as we go along the loop. Recently it has been argued that the exponent associated with the correlation function that measures the probability that two points belong to the same contour loop of a random Gaussian surface is independent of the stiffness ($2\pi g$), and equal to $\frac{1}{2}$ [24]. Therefore, we conclude, that in the $n = 2$ FPL model is $x_2 = \frac{1}{2}$. The numerical result of Blöte and Nienhuis is $x_2 = 0.470(1)$ (see table 1 in [7]), and $x_2 = \frac{1}{2}$ was also found from the Bethe ansatz solution [8].

In the interface representation of the three-colouring model the dimension x_2 can also be associated with a vortex–antivortex correlation function with the magnetic vector charge

$$\boldsymbol{b}_2 = \boldsymbol{B} - \boldsymbol{C} = (0, 1). \tag{15}$$

This comes about in the following way. The correlation function that measures the probability that two points separated by $\boldsymbol{r}$ belong to the same BC loop is $Z(\boldsymbol{r})/Z_0$. The restricted partition function $Z(\boldsymbol{r})$ is simply the number of colourings with a BC loop passing through $\boldsymbol{0}$ and $\boldsymbol{r}$, while Z_0 is the total number of colourings. Now, if we exchange the two colours on the loop along one half of the loop going from $\boldsymbol{0}$ to $\boldsymbol{r}$, then this will generate a vortex and an antivortex with charges $\pm\boldsymbol{b}_2$, at these two points. The dimension x_2 is therefore

$$x_2 = x(\boldsymbol{b}_2). \tag{16}$$

Earlier we found $x_2 = \frac{1}{2}$, and from equation (14) we can now calculate the *exact* value of the coupling in the $n = 2$ FPL model:

$$g = 1. \tag{17}$$

Huse and Rutenberg [15] deduced the value of the coupling constant g for $n = 2$ from the exact solution of the three-colouring model due to Baxter [14]. They showed that from Baxter's solution one can conclude that the interface model is *exactly* at its roughening transition. In standard scaling terms this means that the dimension of the locking potential, $V(\boldsymbol{h})$ in equation (4), is 2. This on the other hand leads to the equation $x(\boldsymbol{G}_{\rm V}) = 2$, where

$\boldsymbol{G}_{\mathrm{V}}$ is the electric vector charge associated with the most relevant vertex operator appearing in the Fourier expansion of the operator $V(\boldsymbol{h})$; $\boldsymbol{G}_{\mathrm{V}}$ is also the second shortest vector in $\mathcal{R}^*$. From equation (11) and $|\boldsymbol{G}_{\mathrm{V}}| = 2$ the value of the coupling, $g = 1$, follows.

Another dimension that was measured by Blöte and Nienhuis is the *temperature dimension* which is associated with a vertex of the honeycomb lattice not covered by a loop. An uncovered vertex becomes, in the three-colouring model, a defect with the same colour on all three of its surrounding bonds [10]; in the interface representation this becomes a vortex with a topological charge†

$$\boldsymbol{b}_{\mathrm{t}} = 3\boldsymbol{A} \tag{18}$$

which is the second shortest vector in $\mathcal{R}$. Hence, using equation (14) for the dimension of a magnetic-type operator, and equation (17) for the value of the coupling, the temperature dimension is

$$x_{\mathrm{t}} = x(\boldsymbol{b}_{\mathrm{t}}) = \tfrac{3}{2}. \tag{19}$$

For comparison, the numerical transfer matrix result is $x_{\mathrm{t}} = 1.46(1)$ (see table 1 in [7]), and it is in good agreement with our exact result when systematic errors are taken into account [7]. This dimension was not calculated by Batchelor *et al* [8].

One possible generalization of the loop correlation function is the so-called *watermelon* correlation function which measures the probability of having m loop segments meeting at two points separated by $\boldsymbol{r}$ [11]; $m = 2$ would then be the loop correlation function. The central result of the Bethe ansatz solution of the FPL model by Batchelor *et al* [8] was the calculation of the watermelon dimensions x_m. Here we show how they can be calculated from the Coulomb gas.

In a way that is completely analogous to the above analysis of the loop correlation function, the watermelon correlator becomes a vortex–antivortex correlation function. Therefore, in order to calculate x_m we need to determine the appropriate magnetic vector charges $\boldsymbol{b}_m$. We divide this calculation up into four steps:

(i) $m = 1$. This corresponds to having a single BC loop segment between points $\mathbf{0}$ and $\boldsymbol{r}$, which in turn implies that the colour configuration at $\mathbf{0}$ is $\{A, A, B\}$. Using the height rule around $\mathbf{0}$ we find

$$\boldsymbol{b}_1 = 2\boldsymbol{A} + \boldsymbol{B} = \left(\frac{\sqrt{3}}{2}, \frac{1}{2}\right). \tag{20}$$

(ii) $m = 2$. In this case there is a BC loop originating at $\mathbf{0}$ and ending at $\boldsymbol{r}$. The associated topological charge was found earlier, equation (15),

$$\boldsymbol{b}_2 = (0, 1). \tag{21}$$

(iii) $m = 2k$. Here we have k BC loops originating in the neighbourhood of $\mathbf{0}$ and ending in the neighbourhood of $\boldsymbol{r}$. The total topological charge around the endpoints is

$$\boldsymbol{b}_{2k} = k\boldsymbol{b}_2. \tag{22}$$

(iv) $m = 2k-1$. This case can be thought of as having $k-1$ BC loops and an additional BC segment, originate in the neighbourhood of $\mathbf{0}$, and end in the neighbourhood of $\boldsymbol{r}$. The total topological charge is

$$\boldsymbol{b}_{2k-1} = (k-1)\boldsymbol{b}_2 + \boldsymbol{b}_1 \tag{23}$$

where $\boldsymbol{b}_1$ and $\boldsymbol{b}_2$ are given by (20) and (21), respectively.

† Here, and throughout, we take the loops in the FPL model to be BC coloured. Of course any other choice of a colour pair would lead to the same results.

Using the exact value of the coupling, $g = 1$, and the above calculated magnetic vector charges, from equation (14) we find for the watermelon dimensions:

$$\begin{aligned} x_{2k} &= \tfrac{1}{2}k^2 \\ x_{2k-1} &= \tfrac{1}{2}(k^2 - k + 1). \end{aligned} \tag{24}$$

These exponents form a special case of the more general spectrum of exponents associated with all the possible magnetic vector charges in the repeat lattice $\boldsymbol{b}_{j,k} = j(\boldsymbol{A} - \boldsymbol{B}) + k(\boldsymbol{A} - \boldsymbol{C}) \in \mathcal{R}$

$$x_{j,k} = x(\boldsymbol{b}_{j,k}) = \tfrac{1}{2}(j^2 + k^2 + jk) \tag{25}$$

where we have once again made use of equation (14). These charges are associated with defects in the FPL model, in which the full-packing constraint is violated locally. Each defect can be contained in a non-selfintersecting polygon on the triangular lattice, dual to the original honeycomb lattice. The edges of the honeycomb lattice cut by the polygon will be called *defect edges*.

The topological charge of a defect in the solid-on-solid version of the model is the vector sum of the height differences measured along the polygon in, say the clockwise direction. This trivial procedure yields via equation (25) the exponent governing the spatial decay of correlations between two oppositely charged defects. In the three-colouring model the charge of a defect is simply that of the corresponding height configuration.

In the loop version of the model two-defect correlations are defined by the requirement that specified defect edges of the two defects be connected by a loop segment, and that the remaining edges be empty. Like everywhere else in the lattice the empty edges correspond to the colour A and the occupied ones to B or C. The possibility of a loop segment connecting defect edges of the same defect must be excluded. This can be done by maximizing the charge of the defect using the choice between B and C for the occupied edges. Thus the corresponding topological charge of the one defect can be found by associating the vector $\boldsymbol{A}$ or $-\boldsymbol{A}$ to the empty defect edges and $\boldsymbol{B}$ or $-\boldsymbol{C}$ to the occupied ones. For the other defect the same rule applies with $\boldsymbol{B}$ and $-\boldsymbol{C}$ replaced by $\boldsymbol{C}$ and $-\boldsymbol{B}$.

It should be noted that the two sublattices of the honeycomb lattice are not equivalent when positioning a defect. For instance, according to the above rule the charge of a vertex with three empty edges is $3\boldsymbol{A}$ on the one sublattice but $-3\boldsymbol{A}$ on the other. Two such defects have a total charge zero only if they are placed on different sublattices. With periodic boundary conditions, correlation functions between two defects that do not have opposite charge are zero. However, with open boundary conditions there are non-zero two-point correlations between different magnetic defects; for defect charges $\boldsymbol{b}$ and $\boldsymbol{b}'$ the exponent is $x(\boldsymbol{b}) + x(\boldsymbol{b}') - x(\boldsymbol{b} + \boldsymbol{b}')$.

4.2. FPL model for $n < 2$

Here we extend the Coulomb-gas description of the FPL model for loop fugacities $n < 2$. We show that this can be accomplished by introducing a background vector charge. The effect of the background charge is a lowering of the conformal charge, and a shift in the scaling dimensions found above.

Let us first introduce, in the three-colouring model, the staggered chirality $\chi(\boldsymbol{r})$. This operator takes two values: it is $+1$ (-1) if the colours go clockwise around the vertex $\boldsymbol{r}$ on the even (odd) sublattice of the honeycomb lattice, and -1 $(+1)$ if the colours go anti-clockwise. For $n < 2$ the action (6) has an extra imaginary bulk term conjugate to the $\chi(\boldsymbol{r})$; this term was introduced in the colouring model by Baxter [14]. The effect of the

bulk term $i\lambda \int d^2\boldsymbol{r}\, \chi(\boldsymbol{r})$, is to assign a phase factor $\exp(\pm i\lambda)$ every time a loop in the FPL model makes a left or a right turn. This will have the effect of assigning to each loop a weight

$$n = e^{-i6\lambda} + e^{i6\lambda} = 2\cos(6\lambda) \tag{26}$$

due to the fact that the difference between the number of left and right turns, when walking along a closed loop on the honeycomb lattice, is six. By inspection of the ideal state graph in figure 2 we conclude that the most relevant vertex operator appearing in the Fourier expansion of $\chi(\boldsymbol{r})$ has an electric vector charge $\boldsymbol{G}_\chi$, which is the second largest vector in $\mathcal{R}^*$ (same as for the locking potential). Therefore at fugacity $n = 2$ the scaling dimension of the chirality is 2, i.e. it is marginal. We expect that its only effect on the Gaussian action f in equation (6) will be an isotropic change of the coupling g†.

Other than the marginal term, the shift of the loop fugacity away from $n = 2$ will also generate a term in the action which couples the height field to the scalar curvature [25]. This can be most readily understood by taking the FPL model to be defined on a cylinder of circumference L. Namely, a seam running along the length of the cylinder has to be introduced in order to give the correct fugacity (n) for loops winding around the cylinder. A bond of colour $\sigma \in \{\boldsymbol{A}, \boldsymbol{B}, \boldsymbol{C}\}$ which crosses the seam gets an extra factor $\exp(i2\pi \boldsymbol{E}_0 \cdot \sigma)$, where the vector charge

$$-2\boldsymbol{E}_0 = (0, -2e_0) \tag{27}$$

is the background charge in the Coulomb gas [13]. The value of $\boldsymbol{E}_0$ is chosen in such a way so that only the B and C bonds acquire a phase $(\pm\pi e_0)$ when crossing the seam. As a reminder, we note that the BC loops in the three-colouring model were chosen earlier to represent the loops of the FPL model; this choice is of course arbitrary, and any one of the three possible choices of colour pairs would give the same results. Summing over the two possible ways of colouring a BC loop, we find for the fugacity of loops winding around the cylinder:

$$n = 2\cos(\pi e_0) \tag{28}$$

which when compared to equation (26) gives the relation

$$\pi e_0 = 6\lambda. \tag{29}$$

The effective-field theory in the presence of the seam can be written as [26]:

$$f = \int d^2\boldsymbol{r}\, \pi g(|\nabla h_1|^2 + |\nabla h_2|^2) + 2\pi i e_0(h_2(L, \infty)) - (h_2(L, -\infty)). \tag{30}$$

This modification of the Gaussian field theory results in a shift of the conformal charge,

$$c = 2 - 6\frac{e_0^2}{g} \tag{31}$$

and it also has an effect on the scaling dimensions of operators. As shown by Dotsenko and Fateev [13], the correlation functions of the modified Coulomb gas can be expressed in terms of correlation functions in the Gaussian model given by equation (6). The non-zero two-point functions in the modified theory are those of vertex operators having opposite electro-magnetic charge in combination with a floating charge $2\boldsymbol{E}_0$ which precisely cancels the background charge $-2\boldsymbol{E}_0$. The floating charge may combine with the negative charge.

† Here we have assumed that the staggered chirality is an integrably marginal operator [23]. This, as will be shown later, is confirmed by Baxter's solution [14].

An operator whose total electromagnetic vector charge is $(\boldsymbol{G}, \boldsymbol{b})$ then has a dimension $x(\boldsymbol{G}, \boldsymbol{b})$ given by [13]

$$x(\boldsymbol{G}, \boldsymbol{b}) = \frac{1}{2g}\boldsymbol{G} \cdot (\boldsymbol{G} - 2\boldsymbol{E}_0) + \frac{g}{2}|\boldsymbol{b}|^2. \tag{32}$$

Instead, the floating charge may split up so that both the positive and negative charge are increased by $\boldsymbol{E}_0$. The dimension of such an operator is given by $x(\boldsymbol{G} + \boldsymbol{E}_0, \boldsymbol{b})$. This is the *complete* spectrum of scaling dimensions in the FPL model, where $\boldsymbol{G} \in \mathcal{R}^*$, $\boldsymbol{b} \in \mathcal{R}$. The background charge is related to the fugacity by equation (28), while the relation between the coupling g and the fugacity n remains unknown. We turn to this problem next.

In the $n = 2$ FPL model the staggered chirality (or equivalently, the locking potential) is marginal. It follows from the exact solution obtained by Baxter [14] that it remains marginal as long as $\exp(\mathrm{i}6\lambda)$ lies on the unit circle, i.e. λ is real. Therefore, the chirality is marginal in the entire regime $0 \leqslant n \leqslant 2$, and one expects it to change the value of the renormalized coupling constant g continuously with n. The dimension of the staggered chirality, for $n < 2$, is governed by the second smallest vector in $\mathcal{R}^*$ *parallel* to $\boldsymbol{E}_0$. Using equation (32) with $\boldsymbol{G}_\chi = (0, 2)$, the marginality of $\chi(\boldsymbol{r})$ (i.e. $x(\boldsymbol{G}_\chi) = 2$) gives the relation between g and e_0:

$$\frac{4 - 4e_0}{2g} = 2 \tag{33}$$

where, from equation (28) we can read off the dependence of the background charge on the fugacity,

$$e_0 = 1 - g = \frac{1}{\pi}\arccos\left(\frac{n}{2}\right). \tag{34}$$

This agrees with the relation obtained numerically by Blöte and Nienhuis [7], and the Bethe ansatz result of Batchelor *et al* [8]. Equipped with equations (32), (33), and (34) we can now calculate the watermelon dimensions x_m for the $n < 2$ FPL model. In the Coulomb-gas representation the watermelon scaling dimensions are given by $x(\boldsymbol{E}_0, \boldsymbol{b}_m)$, where the magnetic charge is given by equation (22) for m even, and by equation (23) for m odd. The electric charge $\boldsymbol{E}_0$ is due to the electric-type operators $\exp(\mathrm{i}2\pi\boldsymbol{E}_0 \cdot \boldsymbol{h})$ that must be inserted at the endpoints of the watermelon configuration in order to correct for the spurious phase factors $\exp(\pm\mathrm{i}6\lambda)$ that arise due to the winding of the loop segments around the endpoints [12]. We conclude that the watermelon scaling dimensions are given by

$$\begin{aligned} x_{2k} &= x(\boldsymbol{E}_0, \boldsymbol{b}_{2k}) = \frac{g}{2}k^2 - \frac{(1-g)^2}{2g} \\ x_{2k-1} &= x(\boldsymbol{E}_0, \boldsymbol{b}_{2k-1}) = \frac{g}{2}(k^2 - k + 1) - \frac{(1-g)^2}{2g} \end{aligned} \tag{35}$$

which was also found by Batchelor *et al* (see equations (16) and (17) in [8]), and it generalizes the $n = 2$ result (24). The dimension x_2 was also calculated numerically by Blöte and Nienhuis [7] for different values of n, and their results agree very well with the exact values.

The temperature dimension x_t, for different values of n, was also determined numerically by Blöte and Nienhuis [7], but this dimension does not appear in the Bethe ansatz solution of Batchelor *et al* [8]. The dimension x_t is related to a defect in the FPL model associated with an uncovered vertex. Unlike the case of the watermelon dimensions there are no loop segments associated with this defect and there is consequently no need for an electric-type

operator to correct for the winding of the loop segments around the endpoints. Therefore, we have

$$x_{\mathrm{t}} = x(0, \boldsymbol{b}_{\mathrm{t}}) = \tfrac{3}{2}g \tag{36}$$

where the magnetic vector charge $\boldsymbol{b}_{\mathrm{t}} = 3\boldsymbol{A}$ (equation (18)). The numerical results in [7] are in very good agreement with our exact result.

Once again the equations (35) and (36) are special cases of a more general spectrum

$$x_{j,k} = \frac{g}{2}(j^2 + k^2 + jk) - \frac{(1-g)^2}{2g}(1 - \delta_{j,k}) \tag{37}$$

for the charge $\boldsymbol{b}_{j,k} = j(\boldsymbol{A} - \boldsymbol{B}) + k(\boldsymbol{A} - \boldsymbol{C})$. These, like equation (25), govern the correlations between mixed defects defined by empty and occupied defect edges and the requirement that the occupied defect edges of both defects are mutually connected. Only for defects with topological charges purely in the $\boldsymbol{A}$ direction is the exponent unaffected by the background charge.

Another way of viewing the effect that the background charge has on the exponents is the following. Consider the transfer matrix of the FPL model on a cylinder of circumference L. In terms of the eigenvalues of the transfer matrix ($\lambda_0 > \lambda_1 > \lambda_2 > \cdots$) the exponents are defined by the gaps between the largest eigenvalue and the smaller ones [26],

$$x_i = \frac{L}{2\pi} \ln \frac{\lambda_0}{\lambda_i}. \tag{38}$$

The free energy of the FPL model is given by the logarithm of the largest eigenvalue, and its finite size scaling is given by

$$f_L = \frac{1}{L} \ln \lambda_0 \simeq f_\infty + \frac{\pi c}{6L^2} \tag{39}$$

where f_∞ is the bulk free energy, and c the central charge. The background charge modifies the ground state of the system through the central charge, equation (31), and therefore the various exponents, corresponding to excited states with respect to this shifted ground state, will also change. In the case of the watermelon dimensions there are extra lines running along the cylinder. This means that for this excited state we should 'turn off' the seam: it is not necessary because loops around the cylinder need not be counted as they are prevented by the lines along the cylinder; moreover a seam is not allowed since it would give a phase factor to the possible (helix-like) winding of these lines. This state will therefore not have the correction from the background charge. As it is measured with respect to the new ground state via equation (38), the watermelon dimension x_m will not only differ from the $n = 2$ value ($x(\boldsymbol{b}_m)$, equation (24)) due to the different value of g, but also by a shift, which is simply $\frac{1}{12}$ of the shift of the central charge in equation (31). Therefore, the value of the watermelon dimensions is

$$x_m = x(\boldsymbol{b}_m) - \frac{6(1-g)^2}{12g} \tag{40}$$

which coincides with equation (35). In the state corresponding to the thermal excitation, loops going around the cylinder are permitted and we need the seam to count those contributions correctly. This state therefore gets shifted in the same way as the ground state. The thermal exponent therefore only differs from the $n = 2$ exponent in the value of g, and is given by equation (36).

5. Geometrical properties of loops

In this section we consider the geometrical properties of loops in the FPL model. We calculate the fractal dimension of loops and the loop-length distribution function.

The length of a loop s, and its radius R are related by

$$s \sim R^{D_f} \tag{41}$$

where D_f is the fractal dimension of the loop. The loop radius is defined as the radius of the smallest circle that contains the loop.

The distribution of loop lengths $P(s)$ measures the probability that a loop, in a fully packed configuration, passing through a chosen vertex has length s. It is given by a power law:

$$P(s) \sim s^{-(\tau-1)}. \tag{42}$$

The geometrical exponents D_f and τ can be related by a scaling argument to the exponent x_2 [27, 5]

$$D_f = 2 - x_2 \qquad \tau - 1 = \frac{2}{2 - x_2}. \tag{43}$$

Using the calculated value of x_2, equation (35), we find:

$$D_f = 1 + \frac{1}{2g} \qquad \tau - 1 = \frac{4g}{1 + 2g}. \tag{44}$$

In the limit $n \to 0$ ($g = \frac{1}{2}$) we find $D_f = 2$, which is what we expect for Hamiltonian walks. For $n = 2$ we find $D_f = \frac{3}{2}$ which is the fractal dimension of equal height (contour) loops on a random Gaussian surface [24]. Indeed, for $n = 2$ the background charge is equal to zero and the action f defines a random Gaussian surface; the loops in the FPL model are contour loops of this random surface. (More precisely, a particular component of the height z does not change along the loop [19].)

In the Kagomé Potts model representation of the $n = 2$ FPL model the exponent $\tau - 1$ has been determined numerically to be 1.34 ± 0.02 [28], in good agreement with the exact result $\tau - 1 = \frac{4}{3}$ which follows from equation (44) for $g = 1$.

6. Summary and remarks

We have calculated the conformal charge and the exact exponents in the fully packed loop model on the honeycomb lattice. To this end we proposed a simple conformal field theory for the scaling limit of this model, and it is given by the vacuum phase of a two-dimensional Coulomb gas with an added background charge. The magnetic and electric charges of the Coulomb gas were found to be *vectors* in the triangular lattice $\mathcal{R}$ (the so-called 'repeat' lattice) and its dual $\mathcal{R}^*$. These charges give the complete operator spectrum of the FPL model, of which the watermelon dimensions calculated by Batchelor *et al* [8] are a subset. The exact value of the temperature dimension found here and not in the Bethe ansatz solution are in agreement with the numerical results of Blöte and Nienhuis [7].

Coulomb-gas methods with vector charges have been used previously by Fateev and Zamolodchikov [29] to calculate correlation functions in the $\mathbb{Z}_3$ models. Their work was extended by Pasquier [30] who considered the continuum limit of lattice models with quantum group symmetries. The FPL model is most likely related to the models of Fateev and Zamolodchikov [29] since in the $n \to 2$ limit the FPL model has an enlarged chiral symmetry, given by the $su(3)_{k=1}$ Kac–Moody algebra [19]. This is also true of the $\mathbb{Z}_3$

models. Moreover, for $n < 2$ we introduced a term proportional to the staggered chirality into the free-energy (action) of the FPL model. The presence of this term breaks the full permutation symmetry of the three-colouring model down to $\mathbb{Z}_3$; only cyclic permutations of the colours leave the staggered chirality unchanged.

Finally, it is interesting to note that in the folding model the microscopic heights $\boldsymbol{z}(\boldsymbol{r})$ specify the *positions* of the vertices $\boldsymbol{r}$, of the triangular lattice in the folded state. The coarse-grained action (entropic in origin), corresponding to the different ways of folding the triangular lattice, is Gaussian; equation (6). In the theoretical considerations of tethered membranes this is usually the starting assumption which is justified by the results of numerical simulations [31]. We see that in this simple folding model the gradient squared form of the entropic contribution to the free energy of folding, is closely related to the fact that the FPL model maps to the vacuum phase of a two-dimensional Coulomb gas.

The ideal states we had identified in the three colouring model are the states that are entropically selected. They are flat, $\boldsymbol{h} =$ constant, and in the folding model they map to states in which the whole triangular lattice has been folded down to a single triangle. Introducing an energy penalty associated with folding might stabilize a flat state of the membrane at low temperatures, while the entropically selected folded states would necessarily win at high temperatures. Therefore, we might expect a *folding transition* to occur at some intermediate temperature. Such a transition was found in the numerical transfer matrix calculation of Di Francesco and Guitter [16]. It would be interesting to study this transition using the Coulomb-gas methods developed here. It is our hope that this will allow us to calculate properties of this intriguing transition exactly.

Acknowledgments

We wish to thank C L Henley and J Cardy for discussions and C L Henley for a careful reading of the manuscript. JK acknowledges support by the NSF through grant nos DMR-9357613 and DMR-9214943 and JdG by the Dutch foundation FOM which is part of the foundation NWO.

References

[1] Pasquier V 1987 *Nucl. Phys.* B **285** 162
[2] Warnaar S O, Nienhuis B and Seaton K A 1992 *Phys. Rev. Lett.* **69** 710
Warnaar S O and Nienhuis B 1993 *J. Phys. A: Math. Gen.* **26** 2301
[3] Evertz H G, Lana G and Marcu M 1993 *Phys. Rev. Lett.* **70** 875
[4] Aizenman M and Nachtergaele B 1994 *Commun. Math. Phys.* **164** 17
[5] Cardy J L 1995 *Fluctuating Geometries in Statistical Mechanics and Field Theory* ed F David, P Ginsparg and J Zinn-Justin (New York: Elsevier)
[6] Reshetikhin N Yu 1991 *J. Phys. A: Math. Gen.* **24** 2387
[7] Blöte H W J and Nienhuis B 1994 *Phys. Rev. Lett.* **72** 1372
[8] Batchelor M T, Suzuki J and Yung C M 1994 *Phys. Rev. Lett.* **73** 2646
[9] Kast A 1995 The fully packed loop model *PhD Thesis* University of California at Berkeley; *Preprint* cond-mat/9411132.
[10] Kondev J and Henley C L 1994 *Phys. Rev. Lett.* **73** 2786
[11] Duplantier B 1986 *J. Phys. A: Math. Gen.* **19** L1009
[12] Nienhuis B 1987 *Phase transitions and Critical Phenomena* vol 11, ed C Domb and J L Lebowitz (London: Academic)
[13] Dotsenko Vl S and Fateev V A 1984 *Nucl. Phys.* B **240** 312
[14] Baxter R J 1970 *J. Math. Phys.* **11** 784
[15] Huse D A and Rutenberg A D 1992 *Phys. Rev.* B **45** 7536
[16] Di Francesco P and Guitter E 1994 *Europhys. Lett.* **26** 455; 1994 *Phys. Rev.* E **50** 4418

[17] Kantor Y and Jarić M V 1990 *Europhys. Lett.* **11** 157
[18] Shender E F, Cherepanov V B, Holdsworth P C W and Berlinsky A J 1993 *Phys. Rev. Lett.* **70** 3812
[19] Kondev J and Henley C L 1996 *Nucl. Phys.* B **464** 540
[20] Villain J, Bidaux R, Carton J-P and Conte R 1980 *J. Physique* **41** 1263
[21] Chui S T and Weeks J D 1976 *Phys. Rev.* B **14** 4978
José J V, Kadanoff L P, Kirkpatrick S and Nelson D R 1977 *Phys. Rev.* B **16** 12
[22] Kondev J unpublished
[23] Choudri S and Schwartz J A 1989 *Phys. Lett.* **219B** 291
[24] Kondev J and Henley C L 1995 *Phys. Rev. Lett.* **74** 4580
[25] Foda O and Nienhuis B 1989 *Nucl. Phys.* B **324** 643
[26] Blöte H W J, Cardy J L and Nightingale M P 1986 *Phys. Rev. Lett.* **56** 742
Affleck I 1986 *Phys. Rev. Lett.* **56** 746
[27] Saleur H and Duplantier B 1987 *Phys. Rev. Lett.* **58** 2325
[28] Chandra P, Coleman P and Ritchey I 1993 *J. Physique* I **3** 591
[29] Fateev V A and Zamolodchikov A B 1987 *Nucl. Phys.* B **280** 644
[30] Pasquier V 1988 *Nucl. Phys.* B **295** 491
[31] Kantor Y, Kardar M and Nelson D R 1986 *Phys. Rev. Lett.* **57** 791